ELSEVIER

Earth and Planetary Science Letters 135 (1995) 77–90

EPSL

A mass proportion method for calculating melting reactions and application to melting of model upper mantle lherzolite

Michael J. Walter [a,*], Thomas W. Sisson [b], Dean C. Presnall [c]

[a] *Carnegie Institution of Washington, Geophysical Laboratory and Center for High Pressure Research, 5251 Broad Branch Road NW, Washington, DC 20015-1305, USA*

[b] *US Geological Survey, M5910 345 Middlefield Road, Menlo Park, CA 94025, USA*

[c] *Magmalogy Laboratory, Center for Lithospheric Studies, The University of Texas at Dallas, Box 830688, Richardson, TX 75083-0688, USA*

Received 31 January 1995; accepted 31 July 1995

Abstract

We present a method for calculating quantitative melting reactions in systems with multiple solid solutions that accounts for changes in the mass proportions of phases between two points at different temperatures along a melting curve. This method can be applied to any data set that defines the phase proportions along a melting curve. The method yields the net change in mass proportion of all phases for the chosen melting interval, and gives an average reaction for the melting path. Instantaneous melting reactions can be approximated closely by choosing sufficiently small melting intervals. As an application of the method, reactions for melting of model upper mantle peridotite are calculated using data from the system $CaO–MgO–Al_2O_3–SiO_2–Na_2O$ (CMASN) over the pressure interval 0.7–3.5 GPa. Throughout almost this entire pressure range, melting of model lherzolite involves the crystallization of one or more solid phases, and is analogous to melting at a peritectic invariant point. In addition, we show that melting reactions for small melting intervals (< 5%) along the solidus of mantle peridotite are significantly different from those calculated for large melting intervals. For large melting intervals (> 10%), reaction stoichiometries calculated in CMASN are usually in good agreement with those available for melting of natural peridotite. The coefficients of melting reactions calculated from this method can be used in equations that describe the behavior of trace elements during melting. We compare results from near-fractional melting models using (1) melting reactions and rock modes from CMASN, and (2) constant reactions representative of those used in the literature. In modeling trace element abundances in melt, significant differences arise for some elements at low degrees of melting (< 10%). In modeling element abundances in the residue, differences increase with increase in degree of melting. Reactions calculated along the model lherzolite solidus in CMASN are the only ones available at present for small degrees of melting so we recommend them for accurate trace element modeling of natural lherzolite.

1. Introduction

Basaltic rocks are generated from melting of peridotite in the Earth's upper mantle. Some basaltic rocks, Mid-Ocean Ridge Basalts (MORB) for exam-

* Corresponding author's present address: Institute for Study of the Earth's Interior, Okayama University, Misasa, Tottori-ken 682-01, Japan.

SSDI 0012-821X(95)00148-4

ple, are thought to be the products of near-fractional melting of peridotite [2,3], whereas, other more mafic varieties, such as picrites and komatiites, may be products of high degrees of batch melting (> 20%) [4]. An accurate model for the generation of basaltic rocks requires a knowledge of the melting behavior of model peridotite compositions over a range of conditions of pressure and temperature. It has proven difficult to amass the required information because of experimental difficulties in constraining the complexity of nine-component composition space and, also, because of difficulties in determining melt compositions at low melt fractions. Many approaches have been adopted to overcome these difficulties including (1) phase equilibrium studies in simplified chemical systems of low variance [1,5–7], (2) parameterization of experimentally produced melt compositions that are saturated with mantle peridotite

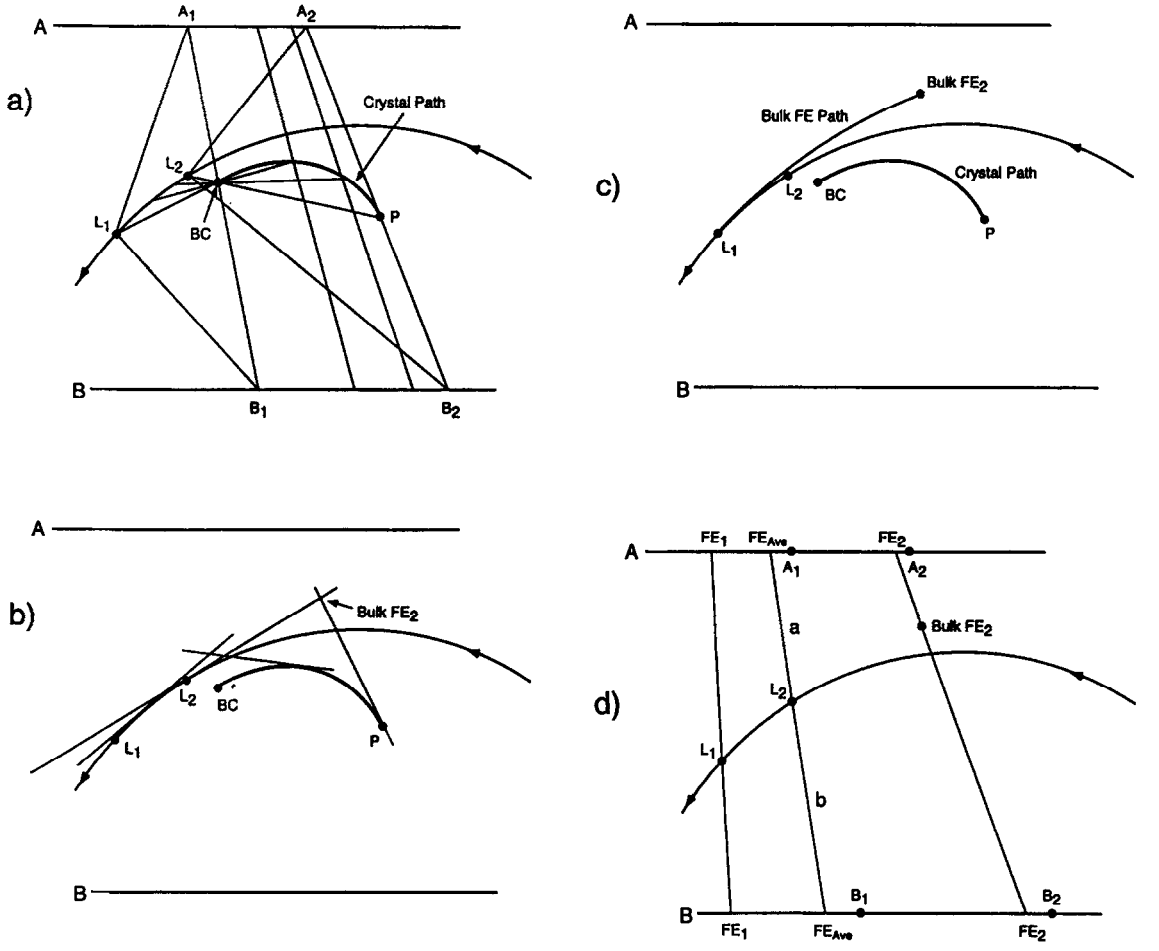

Fig. 1. Hypothetical univariant liquidus boundary line in a ternary system where liquid coexists with phases. A and B of variable composition. (a) Shows tie-lines connecting coexisting phases (e.g., L_1–A_1–B_1) along the liquidus path from L_1 to L_2, and the construction of the crystal path. Arrows on the boundary lines show the direction of decreasing temperature. (b) Shows how the fictive extract at L_2 (i.e., bulk FE_2) is determined as the intersection of a pair of tangent lines; one tangent to the boundary line at L_2 and the other tangent to the crystal path at P. The point, intermediate bulk FE_2, illustrates the construction of a point along the bulk FE path of diagram c. (c) Shows the entire bulk fictive extract path (FE path) and crystal path for the melting interval from L_1 to L_2. (d) Shows the fictive extracts contributed by phases A and B at L_1 (FE_{1A} and FE_{1B}), L_2 (FE_{2A} and FE_{2B}), and the average fictive extracts for the melting interval from L_1 to L_2 ($FE_{\mathrm{Ave}\ A}$ and $FE_{\mathrm{Ave}\ B}$). The mass proportions contributed by phases A and B to the liquid over the melting path from L_1 to L_2 are $(b/a+b)$ and $(a/a+b)$, respectively.

minerals [8,9], and (3) determination of the partitioning behavior of major, minor and trace elements between melt and mantle minerals to calculate melt compositions (the "K_d approach") [10–12]. All of these are powerful approaches and have yielded much information regarding the essentials of basalt generation. Each, however, suffers from uncertainties which, at present, preclude a detailed understanding of basalt generation.

An important piece of information in modeling basalt generation is the "mantle melting reaction" as a function of pressure, temperature and composition of the source. This information is one of the components that can be used to develop more precise models for basalt generation using approaches (2) and (3) listed above. Here, we describe a simple mass balance method that can be used to determine the stoichiometry of melting reactions in systems with multiple solid solutions. We use experimental data from the CMASN system to calculate melting reactions of model upper mantle plagioclase, spinel and garnet lherzolite. These reactions are compared to reactions that have been deduced from melting experiments on natural peridotite compositions, and are used to assess the effect of melting reaction stoichiometry and rock modes on trace element models of basalt generation.

2. Calculation of melting reactions

For melting at an isobaric liquidus invariant point in a known system of n components, the mass proportions of solid phases entering the liquid are easily obtained by writing a balanced equation involving all the $n+1$ coexisting phases [13]. For systems in which melting is not invariant but the compositions of the solid phases do not change with temperature, the mass proportions of phases that crystallize or dissolve upon isobaric cooling or heating can be deduced through the use of the so-called "tangent rule" [14]. However, the tangent method is not strictly applicable in cases where the solid phases change composition with temperature because the composition of the material being transferred from, or to, the crystalline phase is not the same as the composition of that phase [15–17]. When melting is not invariant and the solid phases change composition during melting, another method is required to determine the proportions in which the solid phases contribute their mass to the liquid. The complexities involved in determining equilibrium crystallization and melting paths when one or more of the crystalline phases is a solid solution have been thoroughly treated [5,13,14,18–20]. We present here a mass balance method that builds on these treatments, and results in an accurate determination of the melting reactions that occur during melting of phases that have variable composition in a system of n components. This method requires a knowledge of the proportions of phases in equilibrium along a melting curve.

Fig. 1 shows a univariant boundary line in a hypothetical ternary system along which phases A and B, both solid solutions, coexist with liquid (L). Consider melting of bulk composition BC from point L_1 (solidus) to L_2 (Fig. 1a). It is clear from inspection of the three-phase triangle at L_1 that a liquid composition along this boundary line cannot be described as a linear combination of the coexisting solid phases (i.e., $L_1 \neq A_1 + B_1$). The composition of the material contributed to the liquid by a solid solution at a given point is not the same as the composition of that phase. In the case of equilibrium crystallization, the term fictive extract (FE) has been used by Morse [14] to refer to solid material being extracted instantaneously from the liquid. Here, the fictive extract refers to material being instantaneously extracted from the solids and added to the liquid during equilibrium melting. To determine a melting reaction, one must know the mass proportion of the fictive extract of each phase that contributes to the liquid. The method outlined below, hereafter referred to as the mass proportion method, gives this information.

The locus of crystalline bulk compositions coexisting with liquid along the equilibrium melting path from L_1 to L_2 in Fig. 1 is the crystal path [1] [19]. For a given bulk composition, BC, and three-phase triangle, L_2–A_2–B_2, along the melting path in Fig. 1a, the corresponding point on the crystal path is given by the intersection, P, of two lines. One is the base,

[1] The crystal path of Presnall [19] is equivalent to the total solid composition path as defined by Morse [14].

A_2–B_2, of the three-phase triangle, and the other is a line from L_2 that extends through BC to the line A_2–B_2. The fictive extract contributed to the liquid at L_2 is determined by the intersection of two other lines (see Fig. 1b). One is tangent to the boundary line at L_2; the other is tangent to the crystal path at P. This is evident from the fact that the tangent to the boundary line at L_2 describes the movement of the liquid composition at that point. Therefore, the composition of the crystalline material being added to the liquid that results in this movement must lie along the tangent at L_2. Similarly, the material being extracted from the crystalline bulk composition must lie along the tangent at P. Only one point, bulk FE_2 on Fig. 1b, satisfies both of these constraints. The point bulk FE_2 represents the last material added to the liquid to drive it to L_2, and is the sum of the fictive extracts contributed by phases A and B at L_2. For melting from L_1 to L_2 there is an array of bulk fictive extracts that represents all the instantaneous liquids produced along the melting path (bulk FE path on Fig. 1c).

For melting in a binary solid solution, or in a ternary system with one solid solution, the composition and proportion of the fictive extract is easily deduced by the lever rule directly from the phase diagram. In a system with more than one solid solution, such as that shown in Fig. 1, the liquid at L_2 is the average bulk fictive extract for the entire melting path, and is described in terms of a mixture of two fictive extracts, each representing the average of all the instantaneous fictive extracts contributed to the liquid by phases A and B, respectively, over the melting interval. For example, as melting proceeds from L_1 to L_2, as shown on Fig. 1d, phase A changes composition from A_1 toward A_2 and the initial fictive extract contributed by A has a composition that lies to the left of A_1. The same is true for phase B. The fictive extracts contributed by A and B at L_1 and L_2 are shown as FE_1 and FE_2, respectively, on Fig. 1d. The average of all the fictive extracts contributed by A and B over the melting interval, L_1–L_2, is shown as FE_{Ave}. The mass proportions in which phases A and B each contributed an average fictive extract to the liquid over the melting interval from L_1 to L_2 are obtained as $b/(a+b)$ and $a/(a+b)$, respectively, from the line connecting the average fictive extracts on Fig. 1d. The mass proportions of the average fictive extracts are calculated algebraically as follows. For the melting interval from L_1 to L_2, two mass balance equations are written, one describing the total mass, BC, of the system in terms of the mass proportion of each of the phases that coexist at L_1, and likewise, another equation is written for L_2. In the case shown in Fig. 1:

$$BC = X(L_1) + Y(A_1) + Z(B_1) \quad (1)$$

$$BC = X'(L_2) + Y'(A_2) + Z'(B_2) \quad (2)$$

where X, Y and Z are the mass proportions of phases L_1, A_1, and B_1, and X', Y', and Z' are the mass proportions of phases L_2, A_2, and B_2. In this particular case, BC is at its solidus temperature in Eq. (1), so $X = 0$. However, the method works equally well when BC is initially above its solidus temperature. Removal of subscripts and substitution of Eq. (2) into Eq. (1) yields:

$$(Y - Y')(A) + (Z - Z')(B) = (X' - X)(L) \quad (3)$$

Thus, $Y - Y'$ (ΔY) and $Z - Z'$ (ΔZ) give the mass proportions contributed by A and B (i.e., the mass proportion of the average fictive extracts) to make $X' - X$ (ΔX) of L. Because the total mass of the system is conserved (i.e., $\Delta X + \Delta Y + \Delta Z = 0$) it is irrelevant that phases A_1, B_1 and L_1 (Eq. 1) have compositions different from those of phases A_2, B_2 and L_2 (Eq. 2).

The calculations above give the net change in mass of phases A and B over the entire melting interval from L_1 to L_2, and not the instantaneous reaction at either L_1 or L_2. It is evident from the lines connecting the instantaneous fictive extracts (FE_1 and FE_2) on Fig. 1d that the instantaneous reactions at L_1 and L_2 are very different from the average reaction for the entire melting path. In order to approximate the instantaneous melting reactions with the mass proportion method, the melting interval (i.e., the temperature interval) is simply reduced as much as possible. For example, consider the melting path from L_1 to L_3 in Fig. 2. This diagram shows a portion of the liquid path and crystal path for equilibrium melting of bulk composition BC in a hypothetical ternary system with two solid solutions. The compositions of the solid phases are not shown,

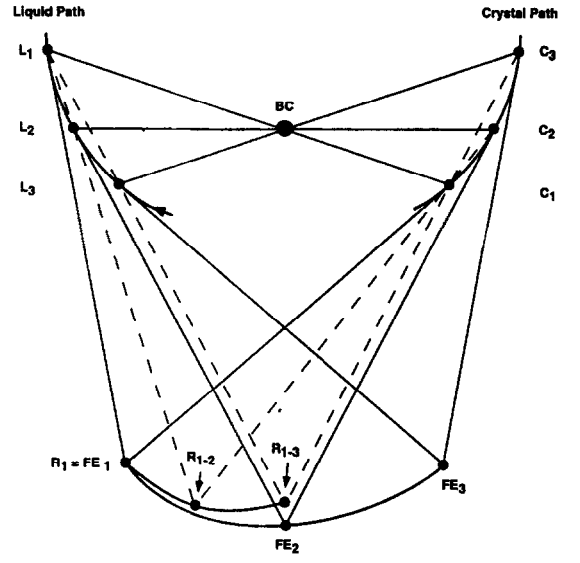

Fig. 2. Hypothetical ternary liquidus diagram showing a portion of the liquid path and crystal path for equilibrium melting of bulk composition BC (diagram after Morse, pers. commun.). The fictive extract path (FE_1–FE_3) has been determined as discussed in the text. The path from FE_1 to FE_3 is the bulk fictive extract path, and the path from R_1 to R_{1-3} is the average bulk fictive extract path. For example, the point R_{1-3} is the average of all the fictive extracts from FE_1 to FE_3. For a given melting interval, such as L_1 to L_3, the average can be found as the intersection of two lines, one projected through L_1 and L_3 and the other projected through C_1 and C_3 (shown as dashed lines). It is the algebraic equivalent of this geometric method that is used to calculate melting reactions. Thus, the mass proportion method gives a net reaction for the melting interval chosen, and the instantaneous reaction that occurs at a given point along a boundary line can only be approached as the temperature interval of melting approaches zero.

and the melting path is highly curved for purposes of illustration. The temperature intervals from L_1 to L_2 and L_2 to L_3 each represent 10% melting and the fictive extract path, FE_1 to FE_3, is determined as described above. The algebraic mass proportion method for calculating a melting reaction, for example from L_1 to L_3, is geometrically equivalent to finding the intersection of the extension of two lines, one projected through L_1 and L_3 and the other projected through C_1 and C_3 (shown as dashed lines in Fig. 2). It is easy to see that the composition at R_{1-3} is not the same as the material being extracted instantaneously at L_1 or L_3 (i.e., FE_1 or FE_3), but is the average of all the fictive extracts produced from L_1 to L_3. Thus, the reaction calculated by mass proportion from L_1 to L_3 is an average reaction. In fact, reactions calculated by the mass proportion method do not depend on the details of the melting path, and only give the net mass change of phases between two points on a melting curve. The reaction yields no information about the rate or direction of mass change (positive or negative) at points along the melting path. However, as the melting interval becomes smaller (e.g., L_1 to L_2) the average fictive extract, R_{1-2}, approaches the instantaneous fictive extract and, at the limit, gives it exactly. In the case where two points along a melting curve are infinitely close ($dT \rightarrow 0$), the mass proportion method yields the exact instantaneous reaction at any point L along a boundary line. For a system having n phases (p), with m fictive extract mass proportions (e), the instantaneous reaction has the general form:

$$de_1 p_1 + de_2 p_2 + \ldots de_m p_n = dx L \qquad (4)$$

In practice, the mass proportion method always gives an average reaction for a melting interval, but the instantaneous reaction can be approached as closely as desired by parameterizing all the phase compositions and choosing a sufficiently small melting interval for the calculation.

3. Lherzolite melting reactions calculated in the system CMASN

In this section, examples are provided that show how the mass proportion method can be used to calculate reactions for melting of model upper mantle lherzolite (olivine + opx + cpx + aluminous phase). For illustration, the experimental data set of Walter and Presnall [1] for melting of model lherzolite in the system CMASN is used. In principle, however, the mass proportion method can be used whenever phase proportions are accurately known over some temperature interval along isobaric lherzolite melting curves.

The compositions of coexisting phases during isobaric univariant melting of model plagioclase and spinel lherzolite in the CMASN system are obtained by using the equations presented in Walter and Pres-

nall [1]. When the compositions of all coexisting phases (four crystalline phases + liquid) are known, their relative mass proportions can be determined accurately for a suitable bulk composition at any temperature along the melting curve by means of the determinant method of Korzhinskii [21] (see also [1,13]). Composition *A* from Walter and Presnall [1] is used as a fertile model lherzolite composition, and a detailed discussion of the equilibrium melting behavior of this composition in the plagioclase and spinel lherzolite stability fields can be found therein.

As an example, consider melting of model lherzolite *A* at 2.0 GPa. To calculate the reaction that occurs at the solidus, two equations are written that describe bulk composition, *A*, in terms of the coexisting phases, one at the solidus, the other 1°C above the solidus:

$$1425.2°C:\ A = 0.00\,\text{liq} + 0.5333\,\text{fo} + 0.1705\,\text{opx} + 0.2676\,\text{cpx} + 0.0286\,\text{sp} \quad (5)$$

$$1426.2°C:\ A = 0.0015\,\text{liq} + 0.5335\,\text{fo} + 0.1709\,\text{opx} + 0.2657\,\text{cpx} + 0.0284\,\text{sp} \quad (6)$$

where, liq is liquid, fo is forsterite, opx is orthopyroxene, cpx is clinopyroxene, and sp is spinel. Substitution of Eq. (6) into Eq. (5), with subsequent rearrangement and renormalization to 1 weight unit of liquid yields the reaction:

$$1.27\,\text{cpx} + 0.13\,\text{sp} = 1.0\,\text{liq} + 0.13\,\text{for} + 0.27\,\text{opx} \quad (7)$$

Eq. (7) describes the net mass of material extracted from cpx and spinel to produce a net increase in the mass of liquid, fo and opx upon heating from 1425.2 to 1426.2°C. Although these temperatures are not experimentally separable, the calculations are meaningful because they are based on parameterized representations of the entire CMASN data set (see [1]). If this procedure is repeated for the temperature interval from 1449.9 to 1450.4°C, the reaction occurring along the melting curve where model lherzolite A has melted to ~ 10% is:

$$0.10\,\text{opx} + 0.96\,\text{cpx} + 0.12\,\text{sp} = 1.0\,\text{liq} + 0.18\,\text{fo} \quad (8)$$

If the interval from 1425.2 (solidus) to 1449.9°C (10% melt) is used, the reaction is:

$$1.04\,\text{cpx} + 0.13\,\text{sp} = 1.0\,\text{liq} + 0.14\,\text{fo} + 0.03\,\text{opx} \quad (9)$$

Table 1
Melting reactions (wt %) calculated at the solidus[1] of model lherzolite A from 0.7 to 3.5 GPa

P (GPa)	opx	cpx	fo	pl	sp	gt	=	liq	opx	cpx	fo	sp	gt
0.7	0.25	0.27	-	0.53	-	-	=	1.0	-	-	0.05	-	-
1.0	0.14	0.28	-	0.58	-	-	=	1.0	-	-	-	-	-
1.3[2]	-	-	0.42	0.97	-	-	=	1.0	0.22	0.06	-	0.11	-
1.7	0.09	0.99	-	-	0.14	-	=	1.0	-	-	0.22	-	-
2.0	-	1.27	-	-	0.13	-	=	1.0	0.27	-	0.13	-	-
2.7	-	1.36	-	-	0.13	-	=	1.0	0.46	-	0.03	-	-
3.0	-	1.43	0.01	-	0.12	-	=	1.0	0.56	-	-	-	-
3.3[3]	3.7	1.9	-	-	1.07	-	=	1.0	-	-	1.0	-	4.67
3.5	-	1.37	0.12	-	-	0.45	=	1.0	0.94	-	-	-	-

[1] The reaction at 3.5 GPa is calculated at ~ 10% melting. Reactions at 1.3 and 3.3 GPa are independent of the amount of melting up to ~ 4% and 8%, respectively. All other reactions are calculated at ≤ 0.5% melting.
[2] Plagioclase to spinel lherzolite univariant transition.
[3] Spinel to garnet lherzolite univariant transition.

Notice the difference between the coefficients in Eqs. (7), (8) and (9). Because the temperature intervals used to calculate Eqs. (7) and (8) were small, these reactions give a close approximation of the instantaneous reactions occurring at ~1425 and 1450°C, respectively. The melting interval used to calculate Eq. (9) gives the net change in mass proportion over a much wider temperature range (~25°C). It does not give the instantaneous reaction at 1450°C, but the net reaction for the interval of melting from 1425 to 1450°C. The choice of how to calculate a reaction depends on the melting process that is being modeled.

Table 1 lists melting reactions calculated at various pressures along the solidus of model lherzolite *A* (see fig. 7 of Walter and Presnall [1]). The reactions occurring along the isobarically univariant portions of the solidus were calculated using the phase proportions determined at two points, one at the solidus, and the other at 1°C above the solidus in the spinel lherzolite field, and 0.1°C above the solidus in the plagioclase lherzolite field. These temperature intervals correspond to melting intervals of about 0.3 and 0.5% for spinel and plagioclase lherzolite melting, respectively. The reactions that take place on the plagioclase to spinel lherzolite and spinel to garnet lherzolite univariant melting curves (listed at 1.3 and 3.3 GPa, respectively) are solved explicitly because the reactions are isobarically invariant. The reaction listed at 3.5 GPa is one in which opx crystallizes and all other phases melt during heating of garnet lherzolite at a temperature above the solidus (see below).

Along the solidus of model lherzolite *A*, melting reactions are, for the most part, peritectic in nature. Forsterite crystallizes during melting at the solidus of plagioclase lherzolite (with the exception of a small pressure range from 1.0 to 1.15 GPa). Along the plagioclase lherzolite to spinel lherzolite transition where isobarically invariant melting occurs (1.15–1.5 GPa), opx, cpx and sp crystallize, while fo and plagioclase (pl) melt during heating. Within the lower pressure portion of the spinel lherzolite field (up to ~1.75 GPa) only fo crystallizes during heating while all other phases melt. At pressures between 1.75 and 3.0 GPa in the spinel lherzolite field, opx and fo crystallize during heating, but at pressures between 3.0 and 3.3 GPa, opx is the only phase to crystallize. Along the spinel to garnet lherzolite univariant melting curve, fo and garnet (gt) crystallize on heating while opx, cpx and sp melt.

On the basis of a single experiment at 3.4 GPa [1] and two unpublished experiments at 4.0 GPa, opx is no longer stable along the solidus of model lherzolite *A* above a pressure of about 3.4 GPa. There is, however, a region above the solidus where opx is produced during melting. The garnet lherzolite melting reaction {liq + opx = fo + cpx + gt} has previously been identified at 3.0 GPa by O'Hara [22] from data along the diopside–pyrope join, at 3.5 GPa by Mysen and Kushiro [23] using data for melting of natural lherzolite, at 5.0 GPa by Herzberg et al. [24] using data from the CMAS system, and at 1.7 GPa by Kinzler [25] using data for melts saturated with natural lherzolite mineral assemblages.

The results above show that melting reactions are sensitive to changes in pressure and temperature (degree of melting) and also, therefore, to bulk composition of the source. Different melting reactions should be used depending on the melting scenario being modeled. A computer program is available from M. Walter to calculate reactions for melting of model plagioclase and spinel lherzolite.

4. Comparisons with melting reactions for natural lherzolite

Two important components missing from the CMASN system that may have a significant influence on melting reactions in natural peridotite systems are FeO and Cr_2O_3. In order to evaluate the effects of addition of these components to CMASN we compare melting reactions from CMASN to those that have been deduced from melting studies on natural peridotite compositions. The only available quantitative assessments of natural peridotite melting reactions are those of Kinzler and Grove [9], Kinzler [25] and Baker and Stolper [26]. Kinzler and Grove presented reactions calculated using a two-liquid procedure that is a multi-component analog to the geometric method of tangents. In this procedure, a mass balance equation is written between a high-temperature liquid along a boundary curve and a lower-temperature liquid on the same boundary curve plus the solids that coexist with the lower-temperature liquid. The two-liquid method is a special case

of our mass balance method that applies rigorously only when the compositions of all the crystalline phases are constant.

We investigated the reliability of the two-liquid method for peridotite systems by calculating melting reactions at 2.0 GPa with data from CMASN, using both the mass proportion method and the two-liquid method at melting intervals ranging from < 1% up to 20% melting of model lherzolite *A*. We found that for a very small melting interval (< 1%) at the solidus, the reactions calculated by the two methods are very different. However, with increasing degree of melting, the two methods yield convergent results. In fact, the reactions calculated from the two methods are nearly identical for a 0–20% melting interval at 2 GPa. We conclude that the two-liquid method is not reliable for determining reactions for small melting intervals, especially near the solidus, but may give reasonable results for large melting intervals. This is not surprising because for small melting intervals, the net composition of the fictive extract contributed to the liquid by a phase of highly variable composition, like cpx in the case of peridotite, is unlike the composition of that phase present initially in the source. However, for a large melting interval in which a phase is nearly consumed, the net composition contributed to the liquid by that phase is close to the composition present initially in the source. In this case, the two-liquid method can give reasonable results. For melting of peridotite over large intervals, the two-liquid method gives results that are comparable to those of the mass proportion method so a direct comparison between reactions calculated in CMASN and those calculated for melting natural peridotite by Kinzler and Grove [9] can be made.

Kinzler and Grove [9] reported melting reactions for plagioclase and spinel lherzolite at 0.9, 1.0, 1.3 and 1.6 GPa. In their study, melting reactions were calculated from their own experiments using pairs of isobaric experiments at different temperatures in which liquid coexisted with a lherzolite assemblage, and also from pairs of experiments reported in the literature [27,28]. While the degree of melting between each pair of experiments could not be specified, the range in *mg#* between the liquids was given, and corresponds in all cases to large melting intervals. Baker and Stolper [26] calculated a lherzolite melting reaction at 1.0 GPa for melting of spinel lherzolite from ~7 to 18 wt% using a method that

Table 2
Comparison of lherzolite melting reactions calculated with data from CMASN (Walter and Presnall [1]) with melting reactions for natural peridotite reported by Kinzler and Grove [9] and Baker and Stolper [26]

P (GPa)	Interval	Method	opx	cpx	fo	pl	sp	=	liq	opx	cpx	fo	pl	sp	ref.
0.9	0 - 25 %	mass prop	0.22	0.26	-	0.53	-	=	1.0	-	-	0.01	-	-	[1]
0.9	*mg#* 65-51	two-liquid	0.18	0.28	-	0.58	-	=	1.0	-	-	0.04	-	-	[9]
1.1	12 - 22 %	mass prop	0.46	0.75	-	-	0.13	=	1.0	-	-	0.34	-	-	[1]
1.0	*mg#* 75-67	two-liquid	0.45	0.76	-	-	0.07	=	1.0	-	-	0.29	-	-	[9]
1.0	~ 7 - 18 %	mass prop	0.38	0.71	-	-	0.13	=	1.0	-	-	0.22	-	-	[26]
1.3	0 - 4%	Korzhinskii	-	-	0.42	0.97	-	=	1.0	0.22	0.06	-	-	0.11	[1]
1.3	*mg#* 58-46	two-liquid	0.84	1.59	-	-	0.19	=	1.0	-	-	0.97	0.63	-	[9]
1.6	2 - 22 %	mass prop	0.25	0.85	-	-	0.12	=	1.0	-	-	0.22	-	-	[1]
1.6	*mg#* 65-51	two liquid	-	1.37	-	-	0.08	=	1.0	0.16	-	0.28	-	-	[9]

is qualitatively similar to the method presented here. We used the mass proportion method to calculate melting reactions for large melting intervals of model lherzolite *A* in CMASN at the same or similar pressures where reactions have been calculated by Kinzler and Grove [9] and Baker and Stolper [26]. The results are presented in Table 2.

At 0.9 GPa, the reaction calculated in CMASN is very similar to the 0.9 GPa reaction (average of 2 reactions in [9]) from natural peridotite, even though the Kinzler and Grove [9] melting reaction was calculated for an Fe-rich portion of the peridotite system. This suggests that the addition of Fe to CMASN does not significantly change melting reactions for plagioclase lherzolite.

At 1.1 GPa, the spinel lherzolite melting reaction in CMASN (12–22% melting) is very similar to that calculated for natural peridotite by Kinzler and Grove [9] (average of 4 reactions in [9]) and Baker and Stolper [26] at 1.0 GPa. The reactions from Kinzler and Grove [9] are based on peridotite melting experiments of Falloon and Green [27] on a MORB + pyrolite composition with an *mg#* appropriate for the Earth's upper mantle.

Baker et al. [29], using the diamond impregnation technique, have reported on the composition of small degree melts of fertile natural spinel lherzolite at 1.0 GPa. They reported that at less than about 7% melting, SiO_2 and Na_2O values increase rapidly and rise as high as 57 and 5.7%, respectively, at 2% melting. While these workers did not report melting reactions, it follows that if melt compositions change rapidly near the solidus then so must melting reactions. Fig. 3 shows the SiO_2 and Na_2O composition of melts for equilibrium melting of model lherzolite *A* at 1.5 GPa in CMASN compared to the results of Baker and Stolper at 1 GPa for natural peridotite. A pressure of 1.5 GPa was chosen for comparison because in the CMASN system at < 1.5 GPa melting begins either on the plagioclase to spinel lherzolite transition curve (1.16–1.5 GPa) or within the plagioclase lherzolite field; between 1.05 and 1.16 GPa the solidus assemblage is plagioclase lherzolite and melting proceeds through the plagioclase–spinel transition and into the spinel lherzolite field (see discussion and fig. 9 in Walter and Presnall [1]). Fig. 3a shows that Na_2O behaves similarly between the two data sets for batch melting of spinel lherzolite. However, Fig. 3b shows that there is a large disparity between the two data sets for SiO_2. As discussed in Walter and Presnall [1], the composition of all phases along isobarically univariant melting curves in CMASN are determined from experiments with high degrees of melting so there is no ambiguity in analyzing phase compositions. The composition of a low-degree melt for a given bulk composition can then be determined accurately by mass balance with a chosen bulk composition [for example, see Eqs. (5) and (6) above]. Baker et al. [29] suggest that the increase in Na_2O in the melt at low melt fractions reduces the activity coefficient of silica in the melt, and that this leads to an increase in silica content. Data in the CMASN system also show that SiO_2 and Na_2O increase as melt fraction decreases, and that the rate of increase of both elements becomes larger

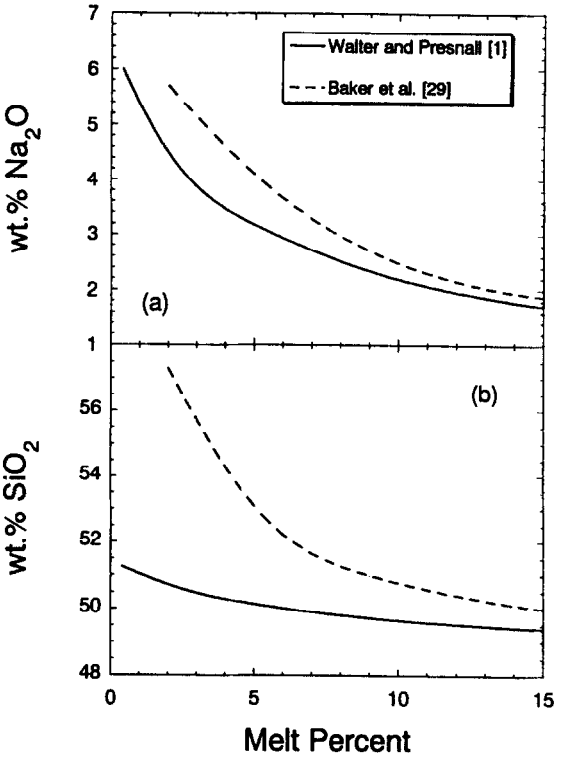

Fig. 3. Wt% Na_2O (a) and SiO_2 (b) vs. melt percent for melting of fertile spinel lherzolite. Solid lines are for melting of model lherzolite A at 1.5 GPa in the CMASN system [1], and dashed lines are for melting of natural lherzolite at 1.0 GPa as reported in Baker et al. [29].

at low melt fractions. Thus, we concur that there appears to be a thermodynamic basis for the correlation of increasing SiO_2 and increasing Na_2O contents. However, in comparison to the data of Baker et al., data from the CMASN system show a much more subdued increase of SiO_2 in the melt It might be argued that the difference in the data sets is due to the absence of Fe in the CMASN system. However, the modeling of Kinzler and Grove [9], which is based on experiments on natural Fe-bearing compositions, shows that high Na_2O (> 5 wt%) melts saturated with natural lherzolite minerals do not have unusually high SiO_2 contents. Further experimental investigation is required to understand the large differences between these data sets.

At 1.3 GPa, the reaction calculated for plagioclase + spinel lherzolite in CMASN has a different form than that calculated by Kinzler and Grove [9] for natural peridotite (average of 3 reactions). In CMASN, the reaction is isobarically invariant and is calculated directly using the method of Korzhinskii [21]. Kinzler and Grove [9] calculate their reactions over an Fe-rich portion of the lherzolite system, with liquid *mg#*'s ranging from 58 to 46 (Table 2), and found that plagioclase crystallizes on heating and spinel is consumed. In contrast, Walter and Presnall [1] showed heating of plagioclase + spinel lherzolite eventually results in the reaction {fo + pl = liq + opx + cpx + sp}, where plagioclase is consumed while spinel crystallizes. Once all plagioclase is consumed, heating to higher temperatures results in melting of spinel lherzolite. Although the presence of a large amount of Fe in the experiments of Kinzler and Grove may account for some of the differences between their reactions and ours, it appears that the complex melting relationships at 1.3 GPa in the CMASN system are not resolved by the data of Kinzler and Grove.

At 1.6 GPa, the CMASN reaction and that calculated for natural peridotite (average of 2 reactions in [9]) are different and, again, take a different form. In CMASN, only fo crystallizes upon heating {opx + cpx + sp = liq + fo}, while in the Kinzler and Grove [9] reaction, opx + ol crystallize on heating {cpx + sp = liq + fo + opx}. However, the melting reaction at the solidus of model lherzolite *A* at ~ 1.75 GPa has the same form as the 1.6 GPa Kinzler and Grove reaction. Further, at ~ 2.3 GPa in CMASN, the coefficients of the 1.6 GPa Kinzler and Grove reaction can be closely matched by calculating the reaction over a large melting interval.

As pointed out in Kinzler and Grove [9], the reactions they listed at 1.6 GPa were calculated with liquids that have *mg#*'s that range from 65 to 51, and so, represent an Fe-rich peridotite system. On the basis of experiments on an Fe-rich spinel lherzolite composition (*mg#* = 75), Bertka and Holloway [30] identified the reaction {cpx + sp = liq + fo + opx} at 1.5 GPa and suggested that the reaction may occur at a pressure as low as 1.0 GPa. Bertka and Holloway discussed in detail how as temperature increases cpx becomes more wollastonite-poor (i.e., enstatite-rich). Kinzler and Grove and Bertka and Holloway recognized that as the composition of cpx becomes more wollastonite-poor with increase in pressure, and therefore, temperature, along the lherzolite solidus, the melting reaction changes from one in which opx dissolves on heating to one in which opx crystallizes. In CMASN, the change in reaction along the solidus at 1.75 GPa, where opx begins to crystallize upon heating, occurs at a wollastonite content in cpx of ~ 20 mol%. More work is needed to determine at what pressure this reaction begins to occur at the solidus of peridotite of upper mantle composition (*mg#* 90). However, on the basis of results from the Fe-rich and Fe-free systems, it is likely to occur in the vicinity of 1.5 GPa.

These comparisons indicate, in general, that (1) for large melting intervals where cpx is nearly consumed, the two-liquid method used by Kinzler and Grove [9] yields results closely similar to the mass proportion method for peridotite systems and can be applied with some confidence to pairs of experiments in which phase compositions are known but phase proportions cannot be determined accurately. It is unlikely that this assumption holds true in all systems where multiple phases have widely variable compositions. (2) This close similarity shows that melting reactions based on data in the CMASN system can be reliably used for modeling melting of natural lherzolite, and (3) because reactions for modeling fractional melting at the solidus are presently not available from data on natural lherzolites, reactions calculated at the model lherzolite solidus in the CMASN system are preferable for modeling of fractional melting processes. These reactions deviate

strongly from reactions applicable to equilibrium melting over larger melting intervals.

5. Effect of melting reaction on trace element modeling

Trace element modeling is used extensively to constrain partial melting processes in the Earth's upper mantle (e.g., [2,10]). The equations presented by Shaw [31] for trace element modeling of partial melting require, as input, the proportions in which coexisting crystalline phases are present in the source, and the proportions, either positive or negative, in which they contribute to the liquid. The general form of the equation used to describe the behavior of a given trace element during equilibrium melting is (e.g., [31]):

$$C_L = \frac{C_S}{D + F(1-P)} \quad (10)$$

where C_L is the trace element concentration in the liquid, C_S is the concentration in the solid before melting, F is the melt fraction, D is the bulk distribution coefficient, and P is the bulk melting coefficient. D is calculated as:

$$D = X_\alpha K^{\alpha/L} + X_\beta K^{\beta/L} + \ldots \quad (11)$$

where X_α is the weight fraction of phase α in the bulk solid, and $K^{\alpha/L}$ is the mineral/melt partition coefficient for the trace element of interest. Similarly, the bulk melting coefficient P is calculated as:

$$P = p_\alpha K^{\alpha/L} + p_\beta K^{\beta/L} + \ldots \quad (12)$$

where p_α is the mass proportion in which phase α has contributed to the liquid. To model a near-fractional melting process in which a small melt fraction is extracted at the solidus, the phase proportions used to calculate the bulk D should be those at the solidus (e.g., Eq. 5), and the melting reaction used to calculate the bulk P should be calculated using an appropriately small melting interval at the solidus (e.g., Eq. 7).

For a trace element with mineral/melt distribution coefficients (D's) that show no significant variation among the phases involved in melting, the stoichiometry of the melting reaction is not important. However, if the D of a trace element varies significantly among the phases present in the source, then the bulk partitioning behavior becomes more sensitive to the proportion of phases in the source, and to the proportions of solid phases that contribute to the melt. We have assessed the sensitivity of trace elements to variations in bulk partition coefficient (D) and bulk melting coefficient (P) by calculating the relative abundances in the melt and residue of a group of seven trace elements for near-fractional melting of spinel lherzolite. In Model 1, we use solidus phase proportions and melting reactions from the CMASN system as input into Eqs. (11) and (12). For comparison, Model 2 is calculated using a constant melting reaction and initial peridotite mode that are representative of what has been used previously in the literature to deduce peridotite melting processes [2,32,33] (see figure caption for details). The selected elements, La, Nd, Hf, Sm, Ti, Dy and Lu, were chosen because they exhibit a range of partitioning behavior, both among lherzolite phases and among elements. Near-fractional melting was adopted because, for a given degree of melting, the effects of variations in bulk D and bulk P on element abundances will be amplified relative to single-step batch melting. The total degree of melting varies from 1 to 10% with melt extracted at 1% increments. Thus, a 10% melt is the average of 10 individual 1% melt extractions. Fig. 4 shows the results for melting of model spinel lherzolite. Plotted on the Y-axis is the relative trace element abundance in Model 2 normalized to Model 1 for both the melt and residue. At 1% melting, relative differences in melt enrichment between the two models range from 17 to 40%. At 5% melting, the differences are reduced to 4–24%, and at 10% melting, < 1–13%. In the residues, relative differences between the models increase with degree of melting. At 1% melting, differences range from 1 to 16%, at 5% melting differences are 2–27%, and at 10% melting, 4–30%. It is important, also, to consider how trace element ratios vary between models because element ratios are often better indicators of petrogenetic processes than individual abundances. At 1% melting, differences in the melt are Lu/Hf ~ 10%, Sm/Nd < 1%, and Ti/Dy ~ 15%. At 10% melting differences are Lu/Hf < 1%, Sm/Nd and Ti/Dy ~ 4%. In the residues, at 1% melting, differences are Lu/Hf ~ 2%, Sm/Nd ~ 3%, and Ti/Dy

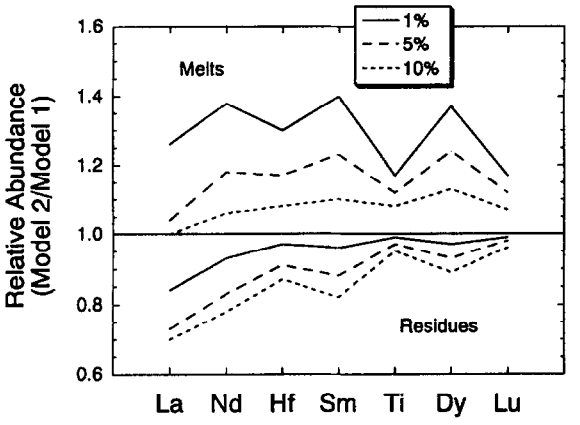

Fig. 4. Relative abundances of trace elements in melt and residue at 1, 5, and 10% near-fractional melting in Model 2 normalized to Model 1. In Model 1, melting is modeled using rock modes and melting reactions as calculated from data in the CMASN system. Melting of spinel lherzolite is assumed to begin at 2.2 GPa and pressure is incremented by 0.1 GPa. At each pressure, the phase proportions are calculated at the solidus from phase equilibrium data (see Eq. 5, for example) and the melting reaction is calculated for the melting increment from 0 to 1%. 1% melt is extracted at each pressure as an approach to fractional melting. Bulk D's and bulk P's are calculated using Eqs. (11) and (12), mineral/melt partition coefficients are as given in [34], and trace element abundances are calculated from Eq. (10). In Model 2, the same procedure is used except that the initial rock mode and the melting reaction are taken from the literature [2] and are representative of values used in other recent studies (e.g., [32,33]). In Model 2, the melting reaction is constant throughout, and the residue is calculated incrementally from the melting reaction only, with no account made for changes in phase proportion as a result of changes in pressure and temperature.

~ 2%. At 10% melting, differences in the residues are Lu/Hf ~ 10%, Sm/Nd ~ 7%, and Ti/Dy ~ 6%. For Sm/Nd and Lu/Hf, these differences are large compared to measurement errors for the isotope dilution technique which is often used to measure these ratios [32].

The results of this single model illustrate that errors derived by assuming an inappropriate melting reaction coupled with an erroneous rock mode can contribute significantly to uncertainty in the model calculations for some elements. For modeling at low degrees of melting (< 10%), which may characterize some "plume" magmas [35,36], errors can be large for the abundance of elements in the melt. When calculating the abundances of elements in melt at the higher degrees of melting that characterize magmas such as some MORBs [2,32], uncertainties associated with measured or calculated partition coefficients and/or trace element measurements in the rocks are probably larger than uncertainties derived from melting reactions and rock modes. Conversely, modeling element abundances in residues becomes more sensitive to melting reactions and rock modes with increase in degree of melting. The errors in any given model will depend critically on what information is used in the model. If partition coefficients with large uncertainties are used to model the abundances of trace elements that also have large analytical uncertainties, then correct melting reactions are unimportant. However, if the highest possible precision is desirable then an effort should be made to use the best available melting reactions and peridotite rock modes. [2]

6. Concluding remarks

The mass proportion method for calculating melting reactions is best used in conjunction with data of the type given by Walter and Presnall [1] for melting of model lherzolite in the CMASN system. These data have a unique advantage not shared by melting experiments on natural compositions. Within the pressure–temperature composition limits of the data set, a complete algebraic description of phase relationships in the 5-component system is provided. This means that for an arbitrarily selected pressure and source composition, calculation of the reactions

[2] It is important to note that the mass proportion method describes the liquid composition in terms of mass proportions of the crystalline phases present in the source, but the compositions of the average fictive extracts that describe the liquid composition are necessarily not the same as those in the source. Therefore, when using reactions calculated by the mass proportion method in trace element modeling equations, an error is introduced if the partition coefficient of the trace element of interest is a strong function of phase composition over the melting interval used to calculate the reaction. If the partitioning of a trace element does show a strong compositional dependence, then calculation of a melting reaction over progressively smaller temperature intervals (approaching fractional melting) will give increasingly precise results.

for an arbitrarily small amount of melting ($\ll 1\%$) precisely at the solidus can be accomplished without any extrapolation of the data from experiments on large amounts of melting. However, the method can also be applied to data on natural compositions as long as phase proportions are known accurately at different temperatures along a melting path. If the compositions of all coexisting phases in melting experiments on natural upper mantle peridotite are determined accurately, then it is possible to calculate phase proportions during melting through mass balance between the system bulk composition and the coexisting phase compositions. Such information could then be parameterized and extrapolated to the peridotite solidus, and the mass proportion method could be used to calculate melting reactions for any desired melting interval.

As our understanding of the partitioning behavior of trace elements during peridotite melting becomes more refined, the manner in which proportions of phases change during melting becomes increasingly important. Accurate modeling of a complex polybaric lherzolite melting process requires the calculation of a specific series of melting reactions that corresponds to a particular pressure–temperature–bulk composition path of a parcel of mantle. While at present, reactions cannot be calculated for such a path from the data for melting of natural lherzolite, they can be calculated using data of Walter and Presnall [1] for model lherzolite in the CMASN system.

Acknowledgements

The authors thank S.A. Morse for comments that significantly improved the manuscript and for the suggestion and permission for us to use Fig. 2. Comments by D. Bell, E. Hauri, H. Yoder, and C. Uellmer are appreciated. Reviews by R.J. Kinzler and K. Hirose are gratefully acknowledged. This work was supported by NSF grants EAR-8816044 and EAR-9219159, and Texas Advanced Research Program grants 009741-007, 009741-066, and 009741-044 to Presnall. Walter acknowledges support from a Killam Foundation Scholarship while at the University of Alberta, and support from the Geophysical Laboratory and Center for High-Pressure Research where the manuscript was prepared. [*CL*]

References

[1] M.J. Walter and D.C. Presnall, Melting behavior of simplified lherzolite in the system $CaO–MgO–Al_2O_3–SiO_2–Na_2O$ from 7 to 35 kbar, J. Petrol. 35, 1994.

[2] K.T.M. Johnson, H.J.B. Dick and N. Shimuzu, Melting in the oceanic upper mantle: an ion microprobe study of diopsides in abyssal peridotite, J. Geophys. Res. 95, 2661–2678, 1990.

[3] J.L. Ahern and D.L. Turcotte, Magma migration beneath an oceanic ridge, Earth Planet. Sci. Lett. 45, 115–122, 1979.

[4] C. Herzberg, Depth and degree of melting of komatiites, J. Geophys. Res. 97, 4521–4540, 1992.

[5] N.L. Bowen and J.F. Schairer, The system $MgO–FeO–SiO_2$, Am. J. Sci. 26, 151–217, 1935.

[6] I. Kushiro, The system forsterite–diopside–silica with and without water at high pressures, Am. J. Sci. (Schairer Vol.) 267A, 269–294, 1969.

[7] D.C. Presnall, S.A. Dixon, J.R. Dixon, T.H. O'Donnell, N.L. Brenner, R.L. Schrock, and D.W. Dycus, Liquidus phase relations on the join diopside–forsterite–anorthite from 1 atm. to 20 kbar: their bearing on the generation and crystallization of basaltic magmas, Contrib. Mineral. Petrol. 66, 203–220, 1978.

[8] D. McKenzie, and M.J. Bickle, The volume and composition of melt generated by extension of the lithosphere, J. Petrol. 29, 625–679, 1988.

[9] R.J. Kinzler and T.L. Grove, Primary magmas of mid-ocean ridge basalts 1. Experiments and methods, J. Geophys. Res., 97, 6885–6906, 1992.

[10] C.H. Langmuir, J.F. Bender, J.F. Bence, G.N. Hanson and S.R. Taylor, Petrogenesis of basalts from the FAMOUS area: mid-Atlantic ridge, Earth Planet. Sci. Lett. 36, 133–156, 1977.

[11] Y. Niu and R. Batiza, Chemical variation trends at fast and slow spreading mid-ocean ridges, J. Geophys. Res. 98, 7887–7902, 1993.

[12] C.H. Langmuir, E.M. Klein and T. Plank, Petrological systematics of mid-ocean ridge basalts: constraints on melt generation beneath oceanic ridges, in: Mantle Flow and Melt generation at Mid-Ocean Ridges, Morgan, Blackman and Sinton, eds., pp. 183–280, Am. Geophys. Union, Washington, DC, 1992.

[13] D.C. Presnall, An algebraic method for determining equilibrium crystallization and fusion paths in multicomponent systems, Am. Mineral. 71, 1061–1070, 1986.

[14] S.A. Morse, Basalts and Phase Diagrams, 493 pp., Springer, New York, NY, 1980.

[15] J.W. Greig, E. Jensen and H.E. Merwin, Melting relationships in the system Cu–Fe–S (unpubl. ms.), Carnegie Inst., Washington, DC, 1958.

[16] M. Hillert, Criterion for peritectic and eutectic reactions, J. Iron Steel Inst. 195, 201–204, 1958.

[17] A.L. Boettcher, The system albite–orthoclase–water and albite–orthoclase–quartz–water: chemographic phase relationships, J. Geophys. Res. 85, 6955–6962, 1980.
[18] R.F. Fudali, Experimental studies bearing on the origin of psuedoleucite and associated problems of alkalic rock systems, Geol. Soc. Am. Bull. 74, 1101–1126, 1963.
[19] D.C. Presnall, The geometrical analysis of partial fusion, Am. J. Sci. 267, 1178–1194, 1969.
[20] D.C. Presnall, Algebraic methods for determining directions of decreasing temperature along isobaric liquidus univariant lines, Can. Mineral. 29, 687–692, 1991.
[21] D.S. Korzhinskii, Physicochemical basis of the analysis of the paragenesis of minerals, Consultants Bureau, New York, NY, 1959.
[22] M.J. O'Hara, The join diopside–pyrope at 30 kbars, Yearb. Carnegie Inst. Wash. 62, 116–118, 1963.
[23] B.O. Mysen and I. Kushiro, Compositional variations of coexisting phases with degree of melting of peridotite in the upper mantle, Am. Mineral. 62, 843–865, 1977.
[24] C. Herzberg, T. Gasparik and H. Sawamoto, Origin of mantle peridotite: constraints from melting experiments to 16.5 GPa., J. Geophys. Res. 95, 15,779–15,903, 1990.
[25] R.J. Kinzler, Mantle melting processes at the spinel–garnet transition (17–21 kb), EOS Trans. Am. Geophys. Union 73, 316, 1993.
[26] M.B. Baker and E.M. Stolper, Determining the composition of high-pressure mantle melts using diamond aggregates, Geochim. Cosmochim. Acta 58, 2811–2827, 1994.
[27] T.J. Falloon and D.H. Green, Anhydrous partial melting of MORB pyrolite and other peridotite compositions at 10 kbar: implication for the origin of primitive MORB glasses, Mineral. Petrol. 37, 181–219, 1987.
[28] K.S. Bartels, R.J. Kinzler and T.L. Grove, High pressure phase relations of a near primary high alumina basalt from Medicine Lake Highland, N. California, Contrib. Mineral. Petrol. 108, 253–270, 1991.
[29] M.B. Baker, M.M. Hirschmann, M.S. Ghiorso and E.M. Stolper, Compositions of near-solidus peridotite melts from experiments and thermodynamic calculations, Nature 375, 308–311, 1995.
[30] C.M. Bertka and J.R. Holloway, Pigeonite at solidus temperatures: implications for partial melting, J. Geophys. Res. 98, 19,755–19,766, 1993.
[31] D.M. Shaw, Trace element fractionation during anatexis, Geochim. Cosmochim. Acta 34, 237–243, 1970.
[32] V.J.M. Salters and S.R. Hart, The Hf-paradox and the role of garnet in the source of mid-ocean ridge basalts, Nature 342, 420–422, 1989.
[33] P.B. Kelemen, H.J.B. Dick and J.E. Quick, Formation of harzburgite by pervasive melt/rock reaction in the upper mantle, Nature 358, 635–641, 1992.
[34] E.H. Hauri and S.R. Hart, Correction to "Constraints on melt migration from mantle plumes: A trace element study of peridotite xenoliths from Savai'i, Western Samoa", J. Geophys. Res. 100, 2003, 1995.
[35] S. Watson and D.P. McKenzie, Melt generation by plumes: a study of Hawaiian Volcanism, J. Petrol. 32, 501–537, 1991.
[36] S. Watson, Rare earth element inversions and percolation models for Hawaii, J. Petrol. 34, 763–783, 1993.